

Highlights

Option pricing model under the G-expectation framework

Ziting Pei, Xingye Yue, Xiaotao Zheng

- A comprehensive risk-neutral option valuation framework is formulated within the G-expectation setting, in which the underlying follows a G-geometric Brownian motion. The resulting pricing problem is governed by a fully nonlinear partial differential equation.
- Both explicit and implicit finite-difference discretizations are constructed for the logarithmically transformed equation. Their consistency, stability, monotonicity, and convergence towards the viscosity solution are rigorously established.
- Theoretical analysis and numerical experiments demonstrate that the logarithmic transformation improves efficiency and reduces computational cost.

Option pricing model under the G-expectation framework

Ziting Pei^a, Xingye Yue^{b,c}, Xiaotao Zheng^{b,*}

^a*School of Business, Suzhou University of Science and Technology, Suzhou, 215006, Jiangsu, China*

^b*Center for Financial Engineering, Soochow University, Suzhou, 215006, Jiangsu, China*

^c*School of Mathematical Sciences, Soochow University, Suzhou, 215006, Jiangsu, China*

Abstract

G-expectation, as a sublinear expectation, provides a powerful framework for modeling uncertainty in financial markets. Motivated by the need for robust valuation under model uncertainty, this work develops a unified risk-neutral valuation approach within the G-expectation environment, yielding a nonlinear generalization of the Black–Scholes model, termed the G-Black–Scholes equation. To enhance computational efficiency and reduce numerical cost, we introduce a logarithmic transformation of the asset price, which yields an alternative nonlinear PDE. Based on this transformed formulation, we design both explicit and implicit finite difference schemes that are rigorously demonstrated to be consistent, stable, monotone, and convergent to the viscosity solution. Numerical examples further confirm the accuracy and computational advantages of the proposed methods. Numerical examples further verify that the proposed schemes achieve high accuracy and that the logarithmic transformation relax the stability constraints of explicit schemes and improves computational efficiency.

Keywords: G-expectation, G-geometric Brownian motion, risk-neutral option pricing, explicit method, implicit method, convergence

1. Introduction

Derivative pricing is an important issue in financial theory and practice. The research on how to price options has a long history in finance, which can be traced back to the work of Bachelier in 1900. The evolution of derivative pricing models remained gradual until the breakthrough contributions of Black and Scholes [3] in 1973, which revolutionized option pricing methodology. Under the no-arbitrage assumption, they used the dynamic replication method to obtain the explicit solution for European call options on stocks that do not pay dividends. Subsequently, in 1997, it was honored with the Nobel Prize in Economics.

The Black-Scholes pricing formula has been widely recognized by the academic and industrial communities for its elegant form and simple calculation. However, this pricing

*Corresponding author

Email address: 20234013002@stu.suda.edu.cn (Xiaotao Zheng)

theory itself involves some assumptions that do not align with practices. For example, one of the important assumptions of the Black-Scholes pricing theory is that stock prices adhere to a geometric Brownian motion, with volatility remaining constant. However, practical studies have shown that volatility is not constant and is more likely to be uncertain. More complex models postulate volatility surfaces that span different underlying asset prices and time periods (refer to, for example, Andersen and Brothertonratcliffe [1]; Coleman et al. [5]). Market practitioners typically construct these surfaces by applying implied volatilities calculated via the Black-Scholes model across a broad spectrum of actively traded instruments. An alternative methodology employs stochastic volatility, which posits that volatility itself follows a random walk pattern, as initially proposed by Heston [7]. Stochastic volatility complicates numerical pricing methods by increasing the number of state variables required.

Lyons [8] and Avellaneda et al. [2] independently proposed the uncertain volatility framework. In this approach, it is assumed that the volatility of the underlying asset lies within a specified range of values. As a result, the prices derived from a no-arbitrage analysis are no longer singular. The only calculable elements are the best-case and worst-case prices for a particular long or short position. When an investor takes the worst-case scenario into account, they can protect their position. Even if the actual volatility varies, as long as it remains within the defined range, the investor can ensure a balance that is not negative within the hedging portfolio. By the Feynman–Kac formula, the mathematical formulation of the uncertain volatility model naturally leads to a nonlinear partial differential equation (PDE). For the single-factor uncertain volatility model, Pooley et al. [9] developed numerical algorithms and discussed their convergence properties. For the two-factor case, Ma and Forsyth [10] proposed a fully implicit finite difference scheme that is unconditionally monotone.

Peng [12] proposed the nonlinear G-expectation and presented concepts such as the G-Brownian motion. He established the stochastic integral using G-Brownian motion and obtained the corresponding G-Itô formula. The central limit theorem in the G-framework derived by Peng [13] provides a theoretical basis for describing the price changes of marketable securities with the G-geometric Brownian motion. The G-geometric Brownian motion can be used to characterize the part of stochastic uncertainty.

This paper studies the risk-neutral pricing problem of options under the G-expectation. In this framework, the G-expected returns of both the underlying assets and the options are the risk-free interest rates. The price S_t of the underlying asset is described by the G-geometric Brownian motion, and the price of the option corresponds to a G-expectation. Using the nonlinear Feynman-Kac formula, the option pricing problem is transformed into solving a fully nonlinear PDE. Furthermore, to improve numerical performance, a logarithmic transformation is applied to the price of the underlying asset, and $X_t = \ln S_t$ is introduced. This transformation significantly relaxes the stability constraint and reduces the computational cost of the explicit scheme. Based on the equation of X_t , this paper presents both explicit and implicit numerical schemes for solving the fully nonlinear PDE respectively. The consistency, stability, and monotonicity of the proposed schemes

are rigorously established, thereby guaranteeing convergence to the viscosity solution of the nonlinear PDE. Numerical examples further confirm the accuracy and computational advantages of the proposed methods.

The remainder of this paper is organized as follows. Section 2 establishes the risk-neutral pricing framework under G-expectation, derives the G-Black-Scholes equation, and introduces a logarithmic transformation to obtain an equivalent nonlinear PDE with improved computational properties. Section 3 presents explicit and implicit finite difference schemes for solving the transformed PDE. Section 4 provides rigorous theoretical analysis, proving consistency, stability, monotonicity, and convergence to the viscosity solution, with convergence rate estimates and proof of convergence for the implicit scheme's nonlinear iteration. Section 5 presents numerical experiments confirming the accuracy and computational advantages of the proposed methods. Section 6 concludes the paper.

2. Risk-neutral option pricing under G-expectation

In this section, we establish a risk-neutral option pricing framework under G-expectation. We begin by defining risk neutrality in the nonlinear expectation setting, then construct a G-option pricing model and derive the corresponding G-Black-Scholes equation. Finally, we introduce a logarithmic transformation to obtain an alternative formulation that improves computational efficiency.

Consider a financial market consisting of three fundamental instruments: risk-free bonds, underlying assets (such as stocks), and derivatives (such as options) written on these assets. The risk-free bond grows at the constant rate $r > 0$, while the underlying asset and derivatives are subject to market uncertainty. In the classical linear probability framework, risk neutrality is a well-established concept where all securities in the market earn the risk-free rate of interest r under an appropriately chosen risk-neutral probability measure. This fundamental principle forms the cornerstone of modern derivative pricing theory, ensuring that arbitrage opportunities are eliminated and enabling the unique valuation of contingent claims.

However, in the nonlinear expectation framework, there exists no concept of probability measure, only the nonlinear expectation operator \mathbb{E} . Therefore, we extend the notion of risk neutrality to the G-expectation setting as follows:

Definition 2.1 (Risk-neutral pricing under G-expectation). *In a G-expectation framework where the market is risk-neutral, the G-expected return on all risky securities equals the risk-free rate of interest r . For an underlying asset price process S_t and a derivative process $U(t, S_t)$ in the G-expectation space $(\Omega, \mathcal{H}, \mathbb{E})$, this implies*

$$\mathbb{E} \left[\frac{S_T}{\Gamma_T} \right] = \frac{S_t}{\Gamma_t}, \quad \mathbb{E} \left[\frac{U(T, S_T)}{\Gamma_T} \right] = \frac{U(t, S_t)}{\Gamma_t}, \quad (1)$$

where $\Gamma_t = e^{rt}$ is the risk-free bond. Consequently, under this risk-neutral market, the fair value of the derivative at time $t = 0$ with initial asset price S_0 is given by

$$U(0, S_0) = e^{-rT} \mathbb{E}[U(T, S_T)]. \quad (2)$$

Previous literature has explored option pricing in incomplete markets under the G-expectation framework through hedging strategies [6, 14, 15]. Building upon this foundation, we now formulate a complete risk-neutral pricing framework under the G-expectation.

A fundamental prerequisite for option pricing is establishing the risk-neutral dynamics of the underlying asset. Consider a stock price process $S(t)$ driven by G-geometric Brownian motion in a G-expectation space $(\Omega, \mathcal{H}, \mathbb{E})$ with a symmetric G-Brownian motion B_t :

$$S_t = S_0 e^{rt - \frac{\sigma^2}{2} \langle B \rangle_t + \sigma B_t}, \quad (3)$$

where $S_0 > 0$ is the initial stock price, $r \geq 0$ is the risk-free interest rate, $\sigma > 0$ is the volatility parameter, $\langle B \rangle_t$ denotes the G-quadratic variation of B_t , and $B_t \sim \mathcal{N}(0, [\underline{\Sigma}^2, \overline{\Sigma}^2])$. By Lemma 3.3.4 and Lemma 3.6.1 of [13], it can be shown that the stock price process $S(t)$ is risk-neutral under G-expectation and satisfies:

$$\begin{cases} dS_t = rS_t dt + \sigma S_t dB_t, \\ S_0 = s_0, \end{cases} \quad (4)$$

and

$$\mathbb{E}[S(t)] = S_0 e^{rt}. \quad (5)$$

Given the risk-neutral stochastic process S_t (4) under the G-expectation framework, we define the value function $U(0, s_0)$ of the G-option as:

$$\begin{aligned} U(0, s_0) &= \mathbb{E} \left[e^{-r(T-t)} \phi(S_T) \mid S_0 = s_0 \right] \\ &= e^{-r(T-t)} \mathbb{E} [\phi(S_T) \mid S_0 = s_0], \end{aligned} \quad (6)$$

where $\phi(S_T)$ is the payoff function.

2.1. G-Black-Scholes equation

By the nonlinear Feynman-Kac formula of [13], the value function $U(t, S)$ satisfies the following fully nonlinear PDE:

$$\begin{cases} \frac{\partial U}{\partial t} + rS \frac{\partial U}{\partial S} + \frac{1}{2} \sup_{\Sigma \in [\underline{\Sigma}, \overline{\Sigma}]} \left(\sigma^2 S^2 \Sigma^2 \frac{\partial^2 U}{\partial S^2} \right) - rU = 0, & 0 \leq t \leq T, \\ U(t, S)|_{t=T} = \phi(S). \end{cases} \quad (7)$$

Remark 2.1. When $\phi(S) = \max(S - K, 0)$ (convex) or $\phi(S) = \max(K - S, 0)$ (concave), the equation reduces to the classical Black-Scholes equation. Specifically, for a call option with convex payoff $\phi(S) = \max(S - K, 0)$, equation (7) becomes:

$$\begin{cases} \frac{\partial U}{\partial t} + rS \frac{\partial U}{\partial S} + \frac{1}{2} \left(\sigma^2 S^2 \overline{\Sigma}^2 \frac{\partial^2 U}{\partial S^2} \right) - rU = 0, & 0 \leq t \leq T, \\ U(t, S)|_{t=T} = \max(S - K, 0), \end{cases} \quad (8)$$

while for a put option with concave payoff $\phi(S) = \max(K - S, 0)$, the equation becomes:

$$\begin{cases} \frac{\partial U}{\partial t} + rS \frac{\partial U}{\partial S} + \frac{1}{2} \left(\sigma^2 S^2 \underline{\Sigma}^2 \frac{\partial^2 U}{\partial S^2} \right) - rU = 0, & 0 \leq t \leq T, \\ U(t, S)|_{t=T} = \max(K - S, 0). \end{cases} \quad (9)$$

Remark 2.2. Clearly, when the symmetric G-Brownian motion degenerates to a standard Brownian motion, the uncertainty in Σ vanishes, and the equation (7) reduces to the classical Black-Scholes equation.

2.2. Logarithmic Transformation and Alternative Formulation

After establishing the G-option pricing model under the asset price process S_t and deriving the associated fully nonlinear PDE, to improve computational efficiency, we introduce a logarithmic transformation on the underlying asset by setting $X = \ln S$. The convenience of this calculation is mainly reflected in the explicit difference method. We will elaborate on the advantages of the logarithmic transformation in the numerical analysis of the explicit method in Section 4.

Under this transformation, we formulate an alternative nonlinear PDE given by,

$$\begin{cases} \frac{\partial V}{\partial t} + r \frac{\partial V}{\partial X} + \sup_{\Sigma \in [\underline{\Sigma}, \bar{\Sigma}]} \left[\frac{1}{2} \sigma^2 \Sigma^2 \cdot \left(\frac{\partial^2 V}{\partial X^2} - \frac{\partial V}{\partial X} \right) \right] - rV = 0, & 0 \leq t \leq T, \\ V(t, X)|_{t=T} = \phi(e^X). \end{cases} \quad (10)$$

Remark 2.3. When the symmetric G-Brownian motion degenerates into a classical Brownian motion, equation (10) reduces to the classical result. Moreover, we consider the log-price process X_t ,

$$\begin{cases} dX_t = rdt - \frac{\sigma^2}{2} d\langle B \rangle_t + \sigma dB_t, \\ X_0 = \ln(s_0), \end{cases} \quad (11)$$

the viscosity solution to the nonlinear PDE (10) corresponds to the value function of the following stochastic problem,

$$V(t, x) = \mathbb{E} \left[e^{-r(T-t)} \phi(e^{X_T}) \mid X_t = x \right]. \quad (12)$$

In the following Section 3, we will present explicit and implicit difference methods for solving the nonlinear PDE (10) respectively.

3. Finite difference methods

Without loss of generality (WLOG), we set the volatility parameter $\sigma = 1$. Under this assumption, the asset price dynamics given in (3) can be rewritten as

$$S_t = S_0 e^{rt - \frac{1}{2} \langle B \rangle_t + B_t}. \quad (13)$$

Then PDE (7) becomes

$$\begin{cases} U_t + rSU_S + \frac{1}{2} \sup_{\Sigma \in [\underline{\Sigma}, \bar{\Sigma}]} \Sigma^2 S^2 U_{SS} - rU = 0, \\ U_T = \phi(S). \end{cases} \quad (14)$$

Moreover, we make a substitution of independent variable $t = T - t$ to transform PDE (10) into the Cauchy problem of a fully nonlinear parabolic equation. The PDE (10) can be rewritten as

$$\begin{cases} V_t - rV_X + rV - \frac{1}{2} \sup_{\Sigma \in [\underline{\Sigma}, \bar{\Sigma}]} \Sigma^2 \cdot (V_{XX} - V_X) = 0, \\ V_0 = \phi(e^X). \end{cases} \quad (15)$$

At $X \rightarrow -\infty$, we have the boundary condition

$$V_t = -rV. \quad (16)$$

It is easy to see that the optimal Σ^* is reached at the end of the intervals, depending only on the sign of the difference between the second-order derivative and the first-order derivative, that is,

$$\Sigma^* = \Sigma(V_{XX} - V_X) = \begin{cases} \bar{\Sigma}, & V_{XX} - V_X \geq 0, \\ \underline{\Sigma}, & V_{XX} - V_X < 0. \end{cases} \quad (17)$$

3.1. Discretization

For computational purpose, we confine the problem (15) within a truncated bounded domain,

$$0 \leq t \leq T \text{ and } |X| < L,$$

with artificial boundary condition at the right boundary. For different contracts, the artificial boundary conditions are modified accordingly. Subsequently, the problem is reformulated as

$$\begin{cases} V_t - rV_X + rV - \frac{\Sigma^2(V_{XX} - V_X)}{2} (V_{XX} - V_X) = 0, & t \in (0, T), X \in (-L, L), \\ V|_{t=0} = \phi(e^X), \\ V_t|_{X=-L} = -rV, \\ V|_{X=L} = \varphi(t). \end{cases} \quad (18)$$

Taking an equi-distance partition with a spatial step size $h = 2L/M$, $\Delta t = T/N$, we have grid points $X_i = -L + i * h$, $t^n = n\Delta t$, for $i = 0, \dots, M$, and $n = 0, \dots, N$. Let V_i^n denote the approximate solution at (t^n, X_i) . In this paper, numerical methods are designed to solve PDE (18).

3.2. Explicit difference method

An explicit scheme for equation (18) reads as, for $n = 0, \dots, N - 1$,

$$\begin{cases} \delta_t V_i^{n+1} - r\delta_h V_i^n + rV_i^{n+1} - \frac{\Sigma^2(\delta_h^2 V_i^n - \delta_h V_i^n)}{2} (\delta_h^2 V_i^n - \delta_h V_i^n) = 0, 0 < i < M, \\ V_i^0 = \phi(e^{X_i}), i = 0, \dots, M, \\ \delta_t V_i^{n+1}|_{X_i=-L} = -rV_i^{n+1}, \\ V_i^{n+1}|_{X_i=L} = \varphi^{n+1}, \end{cases} \quad (19)$$

where

$$\delta_t V_i^{n+1} = \frac{V_i^{n+1} - V_i^n}{\Delta t}, \quad \delta_h V_i^n = \frac{V_{i+1}^n - V_{i-1}^n}{2h}, \quad (20)$$

$$\delta_h^2 V_i^n = \frac{V_{i+1}^n - 2V_i^n + V_{i-1}^n}{h^2}. \quad (21)$$

3.3. Implicit difference method

An implicit scheme for equation (18) reads as, for $n = 0, \dots, N - 1$,

$$\begin{cases} \delta_t V_i^{n+1} - r\delta_h V_i^{n+1} + rV_i^{n+1} - \frac{\Sigma^2(\delta_h^2 V_i^{n+1} - \delta_h V_i^{n+1})}{2} (\delta_h^2 V_i^{n+1} - \delta_h V_i^{n+1}) = 0, 0 < i < M, \\ V_i^0 = \phi(e^{X_i}), i = 0, \dots, M, \\ \delta_t V_i^{n+1}|_{X_i=-L} = -rV_i^{n+1}, \\ V_i^{n+1}|_{X_i=L} = \varphi^{n+1}, \end{cases} \quad (22)$$

where $\delta_t V_i^{n+1}$, $\delta_h V_i^{n+1}$, $\delta_h^2 V_i^{n+1}$ take the same forms as in equations (20)-(21). Since (22) is a nonlinear system, an inner iteration is needed to obtain the solution V_i^{n+1} in each time step. Let $V_i^{n+1,k}$ be the k^{th} estimate for V_i^{n+1} , $V_i^{n+1,k}$ is given by the following Picard's iteration,

$$\begin{cases} \delta_t V_i^{n+1,k+1} - r\delta_h V_i^{n+1,k+1} + rV_i^{n+1,k+1} \\ - \frac{\Sigma^2(\delta_h^2 V_i^{n+1,k} - \delta_h V_i^{n+1,k})}{2} (\delta_h^2 V_i^{n+1,k+1} - \delta_h V_i^{n+1,k+1}) = 0, \\ V_i^0 = \phi(e^{X_i}), \\ \delta_t V_i^{n+1,k+1}|_{X_i=-L} = -rV_i^{n+1,k+1}, \\ V_i^{n+1,k+1}|_{X_i=L} = \varphi^{n+1}. \end{cases} \quad (23)$$

4. Numerical analysis for numerical methods

From the work of Barles and Souganidis [4], we know that numerical solution of (19) or (22) converges to the viscosity solution of the PDE (18) if the method is consistent, stable (in the l_∞ norm) and monotone.

We now give the definition of monotonicity. Denote by

$$g_i = g \left(V_i^{n+1}, \{V_k^{n+1}\}_{k \in N_i}, V_i^n, \{V_k^n\}_{k \in N_i} \right)$$

the left-hand side of the difference equation (19) or (22). Here, $N_i = \{i+1, i-1\}$ presents the set of all nearest-neighbor indexes of i .

Definition 4.1. (*Monotonicity*) *The scheme (19) or (22) is monotone if for all i ,*

$$\begin{aligned} & g_i \left(V_i^{n+1} + \epsilon_i^{n+1}, \{V_k^{n+1}\}_{k \in N_i}, V_i^n, \{V_k^n\}_{k \in N_i} \right) \\ & \geq g_i \left(V_i^{n+1}, \{V_k^{n+1}\}_{k \in N_i}, V_i^n, \{V_k^n\}_{k \in N_i} \right), \quad \epsilon_i^{n+1} \geq 0, \end{aligned} \quad (24)$$

and

$$\begin{aligned} & g_i \left(V_i^{n+1}, \{V_k^{n+1} + \epsilon_k^{n+1}\}_{k \in N_i}, V_i^n + \epsilon_i^n, \{V_k^n + \epsilon_k^n\}_{k \in N_i} \right) \\ & \leq g_i \left(V_i^{n+1}, \{V_k^{n+1}\}_{k \in N_i}, V_i^n, \{V_k^n\}_{k \in N_i} \right), \quad \epsilon_i^n, \epsilon_k^{n+1}, \epsilon_k^n \geq 0. \end{aligned} \quad (25)$$

4.1. Monotonicity and Convergence of explicit scheme (19)

Lemma 4.1. (*Consistency*) *The explicit scheme (19) is consistent.*

Proof. Consistency is verified by observing that the equation in (19) tends to the PDE (18) as $h, \Delta t \rightarrow 0$, since the ‘sup’ operation is continuous. \square

Lemma 4.2. (*Monotonicity*) *If condition $\bar{\Sigma} \sqrt{\Delta t} \leq h \leq \frac{2\underline{\Sigma}^2}{\max(2r - \underline{\Sigma}^2, \bar{\Sigma}^2 - 2r)}$ is satisfied, then the explicit scheme (19) is monotone.*

Proof. We first consider the perturbation on V_i^{n+1} , it is obvious from equation (19) that

$$g_i \left(V_i^{n+1} + \epsilon_i^{n+1}, V_i^n, \{V_k^n\}_{k \in N_i} \right) - g_i \left(V_i^{n+1}, V_i^n, \{V_k^n\}_{k \in N_i} \right) \geq 0. \quad (26)$$

We now turn to the perturbation on V_i^n and $\{V_k^n\}_{k \in N_i}$. Denote by $\tilde{V}_i^n = V_i^n + \epsilon_i^n$, for $\epsilon_i^n \geq 0$. We also denote by $\tilde{V}_k^n = V_k^n + \epsilon_k^n$, for $\epsilon_k^n \geq 0$ and $k \in N_i$. Then the difference between the two sides of the inequality (25) is

$$\begin{aligned} T : &= g_i \left(V_i^{n+1}, \tilde{V}_i^n, \{\tilde{V}_k^n\}_{k \in N_i} \right) - g_i \left(V_i^{n+1}, V_i^n, \{V_k^n\}_{k \in N_i} \right) \\ &= -\frac{\epsilon_i^n}{\Delta t} - r \delta_h \tilde{V}_i^n + r \delta_h V_i^n - \frac{\tilde{\Sigma}^2}{2} \cdot \left(\delta_h^2 \tilde{V}_i^n - \delta_h V_i^n \right) + \frac{\hat{\Sigma}^2}{2} \cdot \left(\delta_h^2 V_i^n - \delta_h V_i^n \right) \\ &= -\frac{\epsilon_i^n}{\Delta t} - r \delta_h \tilde{V}_i^n + r \delta_h V_i^n - \frac{\tilde{\Sigma}^2}{2} \cdot \left(\delta_h^2 \tilde{V}_i^n - \delta_h \tilde{V}_i^n \right) + \frac{\hat{\Sigma}^2}{2} \cdot \left(\delta_h^2 \tilde{V}_i^n - \delta_h \tilde{V}_i^n \right) \\ &\quad + \frac{\hat{\Sigma}^2}{2} \cdot \left(\delta_h^2 V_i^n - \delta_h V_i^n \right) - \frac{\tilde{\Sigma}^2}{2} \cdot \left(\delta_h^2 \tilde{V}_i^n - \delta_h \tilde{V}_i^n \right) \\ &\leq -\left(\frac{1}{\Delta t} - \frac{\hat{\Sigma}^2}{h^2} \right) \epsilon_i^n - \left(\frac{r}{2h} + \frac{\hat{\Sigma}^2}{2h^2} - \frac{\hat{\Sigma}^2}{4h} \right) \epsilon_{i+1} - \left(\frac{\hat{\Sigma}^2}{2h^2} - \frac{r}{2h} + \frac{\hat{\Sigma}^2}{4h} \right) \epsilon_{i-1}, \end{aligned}$$

since $\frac{\tilde{\Sigma}^2}{2} \cdot (\delta_h^2 \tilde{V}_i^n - \delta_h \tilde{V}_i^n) \geq \frac{\hat{\Sigma}^2}{2} \cdot (\delta_h^2 \tilde{V}_i^n - \delta_h \tilde{V}_i^n)$, where

$$\tilde{\Sigma} = \Sigma \left(\delta_h^2 \tilde{V}_i^n - \delta_h \tilde{V}_i^n \right), \quad \hat{\Sigma} = \Sigma \left(\delta_h^2 V_i^n - \delta_h V_i^n \right).$$

If condition $\bar{\Sigma} \sqrt{\Delta t} \leq h \leq \frac{2\underline{\Sigma}^2}{\max(2r - \underline{\Sigma}^2, \bar{\Sigma}^2 - 2r)}$ is satisfied, then we obtain $T \leq 0$. The monotonicity of scheme (19) now follows directly from Definition 4.1. \square

Lemma 4.3. (Stability) *If condition $\bar{\Sigma} \sqrt{\Delta t} \leq h \leq \frac{2\underline{\Sigma}^2}{\max(2r - \underline{\Sigma}^2, \bar{\Sigma}^2 - 2r)}$ is satisfied, then the explicit scheme (19) is stable, in the sense that*

$$\max_n \|V^n\|_\infty \leq \max \left(\|\phi\|_\infty, \max_n |\varphi^n| \right). \quad (27)$$

Proof. For notational simplicity, we let $\mathbb{I}_h V_i^n = \delta_h^2 V_i^n - \delta_h V_i^n$, then we can rewrite (19) as the following equation

$$\begin{aligned} V_i^{n+1} = & \frac{1}{1+r\Delta t} \left\{ \frac{\Delta t}{2h} \left(\frac{\Sigma^2 (\mathbb{I}_h V_i^n)}{h} + \frac{\Sigma^2 (\mathbb{I}_h V_i^n)}{2} - r \right) V_{i-1}^n \right. \\ & \left. + \left(1 - \frac{\Sigma^2 (\mathbb{I}_h V_i^n) \Delta t}{h^2} \right) V_i^n + \frac{\Delta t}{2h} \left(r + \frac{\Sigma^2 (\mathbb{I}_h V_i^n)}{h} - \frac{\Sigma^2 (\mathbb{I}_h V_i^n)}{2} \right) V_{i+1}^n \right\}. \end{aligned} \quad (28)$$

Let i_0 be an index such that $|V_{i_0}^{n+1}| = \|V^{n+1}\|_\infty$. Then it is easy to prove that the maximum value cannot be attained at the left boundary. However it may be attained at the right boundary, that is, $i_0 = M$, we have

$$\|V^{n+1}\|_\infty \leq |\varphi^{n+1}|. \quad (29)$$

Then for $0 < i_0 < M$, from the discrete scheme (28) and the condition $\bar{\Sigma} \sqrt{\Delta t} \leq h \leq \frac{2\underline{\Sigma}^2}{\max(2r - \underline{\Sigma}^2, \bar{\Sigma}^2 - 2r)}$, we have

$$\begin{aligned} \|V^{n+1}\|_\infty &= |V_{i_0}^{n+1}| \\ &\leq \frac{1}{1+r\Delta t} \left\{ \frac{\Delta t}{2h} \left(\frac{\Sigma^2 (\mathbb{I}_h V_i^n)}{h} + \frac{\Sigma^2 (\mathbb{I}_h V_i^n)}{2} - r \right) \|V^n\|_\infty \right. \\ &\quad \left. + \left(1 - \frac{\Sigma^2 (\mathbb{I}_h V_i^n) \Delta t}{h^2} \right) \|V^n\|_\infty + \frac{\Delta t}{2h} \left(r + \frac{\Sigma^2 (\mathbb{I}_h V_i^n)}{h} - \frac{\Sigma^2 (\mathbb{I}_h V_i^n)}{2} \right) \|V^n\|_\infty \right\} \\ &\leq \frac{1}{1+r\Delta t} \|V^n\|_\infty \end{aligned} \quad (30)$$

which then results in

$$\|V^{n+1}\|_\infty \leq \frac{1}{(1+r\Delta t)^N} \|\phi\|_\infty. \quad (31)$$

Combining equations (29) and (31) gives

$$\max_n \|V^n\|_\infty \leq \max \left(\|\phi\|_\infty, \max_n |\varphi^n| \right).$$

□

Theorem 4.1. (*Convergence to the viscosity solution*) Suppose the time step Δt and space step h satisfy the stability condition

$$\bar{\Sigma}\sqrt{\Delta t} \leq h \leq \frac{2\underline{\Sigma}^2}{\max \left(2r - \underline{\Sigma}^2, \bar{\Sigma}^2 - 2r \right)},$$

provided that $\max \left(2r - \underline{\Sigma}^2, \bar{\Sigma}^2 - 2r \right) > 0$. Then, the numerical solution generated by the explicit scheme (19) converges to the viscosity solution of the nonlinear PDE (18) as $h \rightarrow 0$.

Proof. Since the scheme (19) is consistent, l_∞ -stable, and monotone, the convergence follows from the results of Barles and Souganidis [4] directly. □

Remark 4.1. An explicit scheme for equation (14) reads as

$$\begin{cases} \delta_t U_i^{n+1} + rS\delta_h U_i^{n+1} + \frac{1}{2}S^2\underline{\Sigma}^2 (\delta_h^2 U_i^{n+1}) \delta_h^2 U_i^{n+1} - rU_i^n = 0, \\ U_i^N = \phi(S_i). \end{cases}$$

It is easy to obtain that the condition for the explicit scheme to converge to the viscosity solution of the nonlinear PDE (14) is

$$S_{\max}\bar{\Sigma}\sqrt{\Delta t} \leq h_s \leq \frac{S_{\min}\underline{\Sigma}^2}{r}, \quad (32)$$

where

$$S_{\max} = e^L, S_{\min} = e^{-L}, h_s = \frac{S_{\max} - S_{\min}}{M}.$$

Then, the constraint for Δt is obtained as

$$\frac{S_{\max}^2 \bar{\Sigma}^2 M^2}{(S_{\max} - S_{\min})^2} \Delta t \leq 1. \quad (33)$$

In contrast, when applying the logarithmic transformation with a fixed number of spatial nodes, the convergence condition established in Theorem 4.1 yields

$$\bar{\Sigma}\sqrt{\Delta t} \leq h_x \leq \frac{2\underline{\Sigma}^2}{\max \left(2r - \underline{\Sigma}^2, \bar{\Sigma}^2 - 2r \right)}, \quad (34)$$

where

$$h_x = \frac{\ln(S_{\max}) - \ln(S_{\min})}{M}.$$

Then, the constraint for Δt is obtained as

$$\frac{\bar{\Sigma}^2 M^2}{(\ln(S_{\max}) - \ln(S_{\min}))^2} \Delta t \leq 1. \quad (35)$$

Combining inequalities (33) and (35), we find that the grid ratio (for time discretization) of the numerical scheme with logarithmic transformation is $\frac{S_{\max}^2(\ln(S_{\max}) - \ln(S_{\min}))^2}{(S_{\max} - S_{\min})^2}$ times lower than that without the transformation. For notational simplicity and when the context is unambiguous, we shall denote h_x as h in the subsequent analysis.

Theorem 4.2. (Rate of convergence) Let v be the viscosity solution of equation (18), V be the numerical solution of equation (19). If condition $\bar{\Sigma}\sqrt{\Delta t} \leq h \leq \frac{2\bar{\Sigma}^2}{\max(2r - \bar{\Sigma}^2, \bar{\Sigma}^2 - 2r)}$ is satisfied and there exists some $\beta \in (0, 1)$, such that $v \in C^{1+\beta/2, 2+\beta}([0, T] \times \Omega)$, then

$$\max_n \|v^n - V^n\|_{\infty} \leq C \left(\Delta t^{\frac{\beta}{2}} + h^{\beta} \right), \quad (36)$$

where C is a positive constant independent of Δt and h .

Proof. Approximating the derivatives by corresponding difference quotients in (18), we obtain

$$0 = \delta_t v_i^{n+1} + R_t^n - r \left(\delta_h v_i^n + \widetilde{R}_h^n \right) - \frac{1}{2} \sup_{\Sigma \in [\underline{\Sigma}, \bar{\Sigma}]} \Sigma^2 \cdot \left(\delta_h^2 v_i^n + R_h^n - \left(\delta_h v_i^n + \widetilde{R}_h^n \right) \right). \quad (37)$$

Here we have the truncation error terms

$$R_t^n = v_t^n - \delta_t v_i^{n+1} = O((\Delta t)^{\beta/2}), \widetilde{R}_h^n = v_x^n - \delta_h v_i^n = O(h^{1+\beta}), R_h^n = v_{xx}^n - \delta_h^2 v_i^n = O(h^{\beta}).$$

Thanks to $\sup(f + g) \leq \sup f + \sup g$, we have

$$\delta_t v_i^{n+1} - r \delta_h v_i^n + r v_i^{n+1} - \frac{1}{2} \sup_{\Sigma \in [\underline{\Sigma}, \bar{\Sigma}]} \Sigma^2 \cdot (\delta_h^2 v_i^n - \delta_h v_i^n) \leq R_{up}^n, \quad (38)$$

where

$$R_{up}^n = -R_t^n + r \widetilde{R}_h^n + \frac{1}{2} \sup_{\Sigma \in [\underline{\Sigma}, \bar{\Sigma}]} \Sigma^2 \cdot \left(R_h^n - \widetilde{R}_h^n \right). \quad (39)$$

By the fact $\sup(f + g) \geq \sup f + \inf g$, we have

$$\delta_t v_i^{n+1} - r \delta_h v_i^n + r v_i^{n+1} - \frac{1}{2} \sup_{\Sigma \in [\underline{\Sigma}, \bar{\Sigma}]} \Sigma^2 \cdot (\delta_h^2 v_i^n - \delta_h v_i^n) \geq R_{low}^n, \quad (40)$$

where

$$R_{low}^n = -R_t^n + r\widetilde{R}_h^n + \frac{1}{2} \inf_{\Sigma \in [\underline{\Sigma}, \overline{\Sigma}]} \Sigma^2 \cdot (R_h^n - \widetilde{R}_h^n). \quad (41)$$

Set $W_i^n = v_i^n - V_i^n$, then we have, by the fact $\sup(f - g) \geq \sup f - \sup g$, that, for $0 < i < M$,

$$\begin{aligned} & \delta_t W_i^{n+1} - r\delta_h W_i^n + rW_i^{n+1} - \frac{1}{2} \sup_{\Sigma \in [\underline{\Sigma}, \overline{\Sigma}]} \Sigma^2 \cdot (\delta_h^2 W_i^n - \delta_h W_i^n) \\ = & \delta_t(v_i^{n+1} - V_i^{n+1}) - r\delta_h(v_i^n - V_i^n) + r(v_i^{n+1} - V_i^{n+1}) \\ & - \frac{1}{2} \sup_{\Sigma \in [\underline{\Sigma}, \overline{\Sigma}]} \Sigma^2 \cdot (\delta_h^2(v_i^n - V_i^n) - \delta_h(v_i^n - V_i^n)) \\ \leq & \delta_t v_i^{n+1} - r\delta_h v_i^n + r v_i^{n+1} - \frac{1}{2} \sup_{\Sigma \in [\underline{\Sigma}, \overline{\Sigma}]} \Sigma^2 \cdot (\delta_h^2 v_i^n - \delta_h v_i^n) \\ & - \left(\delta_t V_i^{n+1} - r\delta_h V_i^n + rV_i^{n+1} - \frac{1}{2} \sup_{\Sigma \in [\underline{\Sigma}, \overline{\Sigma}]} \Sigma^2 \cdot (\delta_h^2 V_i^n - \delta_h V_i^n) \right) \\ \leq & R_{up}^n, \end{aligned} \quad (42)$$

where we have used (19) and (38). Proceeding as in the proof of Lemma 4.3, we have

$$\|W^{n+1}\|_\infty \leq \frac{1}{1 + r\Delta t} \|W^n\|_\infty + \|R_{up}^n\|_\infty,$$

with the initial condition $W_i^0 = 0$, which then results in

$$\|v^{n+1} - V^{n+1}\|_\infty \leq N \|R_{up}^n\|_\infty. \quad (43)$$

Similarly, let $\widetilde{W}_i^{n+1} = V_i^{n+1} - v_i^{n+1}$, then from (40), we have

$$\|v^{n+1} - V^{n+1}\|_\infty \leq N \|R_{low}^n\|_\infty. \quad (44)$$

Hence, we finally have

$$\max_n \|v^n - V^n\|_\infty \leq N * \max_n (\|R_{up}^n\|_\infty + \|R_{low}^n\|_\infty) \leq C((\Delta t)^{\beta/2} + h^\beta).$$

□

4.2. Numerical analysis for Implicit method

The implicit scheme (23) leads to a nonlinear algebraic system which must be solved by an inner iteration at each time step. In this section, we first prove the convergence of the inner iteration and then check the properties of consistence, stability, and monotonicity.

4.2.1. Convergence of inner iteration

Proposition 4.1. (Maximum principle) *If condition $h \leq \frac{2\Sigma^2}{\max(2r-\Sigma^2, \Sigma^2-2r)}$ is satisfied, and $\{V_i^n\}$ satisfies*

$$\mathbb{L}_h V_i^n \equiv \delta_t V_i^n - r\delta_h V_i^n + rV_i^n - \frac{\Sigma^2}{2} \cdot (\delta_h^2 V_i^n - \delta_h V_i^n) \geq 0 (\leq 0), \quad n = 1, \dots, N, \quad 0 < i < M, \quad (45)$$

where $\Sigma \in \{\underline{\Sigma}, \overline{\Sigma}\}$. Then the minimum (maximum) of $\{V_i^n\}$ can only be achieved at the initial or boundary points, unless $\{V_i^n\}$ is constant.

Re-formulate the right-hand side of system (45) into an operator form as

$$\mathbb{L}_h V^n = \left(\frac{1}{\Delta t} I - r\delta_h + r - \frac{\Sigma^2}{2} \cdot \delta_h^2 + \frac{\Sigma^2}{2} \cdot \delta_h \right) V^n - \frac{1}{\Delta t} V^{n-1} \equiv AV^n - \frac{1}{\Delta t} V^{n-1}.$$

It is easy to check that, $A = (a_{ij})$ is an M-matrix, that is, $a_{ii} > 0$, $a_{ij} \leq 0$, for $i \neq j$, and $\sum_{j \neq i} |a_{ij}| < a_{ii}$. Then the above proposition follows.

Theorem 4.3. (Convergence of inner iteration) *If condition $h \leq \frac{2\Sigma^2}{\max(2r-\Sigma^2, \Sigma^2-2r)}$ is satisfied, then for any initial guess $V^{n+1,0}$, the iterative sequence $\{V^{n+1,k}\}_{k>0}$ in (23) iteration is bounded and monotonically increasing, so converges to the unique solution to (22).*

Proof. Denote by $\overline{V}^k = V^{n+1,k}$ and let $W^k = \overline{V}^{k+1} - \overline{V}^k$, $k \geq 1$, then W_i^k satisfies the following difference equation

$$\begin{cases} \frac{W_i^k}{\Delta t} - r\delta_h W_i^k + rW_i^k - \frac{\Sigma^2(\delta_h^2 \overline{V}_i^k - \delta_h \overline{V}_i^k)}{2} (\delta_h^2 \overline{V}_i^{k+1} - \delta_h \overline{V}_i^{k+1}) \\ + \frac{\Sigma^2(\delta_h^2 \overline{V}_i^{k-1} - \delta_h \overline{V}_i^{k-1})}{2} (\delta_h^2 \overline{V}_i^k - \delta_h \overline{V}_i^k) = 0, \\ W_i^k|_{X_i=-L} = 0, \\ W_i^k|_{X_i=L} = 0. \end{cases} \quad (46)$$

Since $\frac{\Sigma^2(\delta_h^2 \overline{V}_i^k - \delta_h \overline{V}_i^k) - \Sigma^2(\delta_h^2 \overline{V}_i^{k-1} - \delta_h \overline{V}_i^{k-1})}{2} (\delta_h^2 \overline{V}_i^k - \delta_h \overline{V}_i^k) \geq 0$, we have

$$\begin{cases} \frac{W_i^k}{\Delta t} - r\delta_h W_i^k + rW_i^k - \frac{\Sigma^2(\delta_h^2 \overline{V}_i^k - \delta_h \overline{V}_i^k)}{2} (\delta_h^2 W_i^k - \delta_h W_i^k) \geq 0, \\ W_i^k|_{X_i=-L} = 0, \\ W_i^k|_{X_i=L} = 0. \end{cases}$$

From the maximum principle, we have $W_i^k \geq 0$, for $0 < i < M$, that is, $\overline{V}_i^{k+1} \geq \overline{V}_i^k$, $k \geq 1$. So $\{\overline{V}_i^k\}_{k>0}$ is a monotonic increasing sequence. Now we check the boundedness of the sequence. From Proposition 4.1, the maximum principle holds for the system (23).

Furthermore, it is easy to prove that the maximum value cannot be attained on the left boundary. It follows that

$$\left\| \overline{V}^{k+1} \right\|_{\infty} \leq \max \left(\|\phi\|_{\infty}, \max_n |\varphi^n| \right). \quad (47)$$

Consequently, as a monotonic and bounded sequence, \overline{V}^k converges. \square

4.2.2. Monotonicity and Convergence of implicit scheme (22)

Lemma 4.4. (Consistency) *The implicit scheme (22) is consistent.*

Proof. The proof process is the same as that in Lemma 4.1, and thus, it will not be reiterated here. \square

Lemma 4.5. (Monotonicity) *If condition $h \leq \frac{2\tilde{\Sigma}^2}{\max(2r-\tilde{\Sigma}^2, \tilde{\Sigma}^2-2r)}$ is satisfied, then the implicit scheme (22) is monotone.*

Proof. Proceeding as in the proof of Lemma 4.2, we first consider the perturbation on V_i^{n+1} , and denote it by $\tilde{V}_i^{n+1} = V_i^{n+1} + \epsilon_i^n$, for $\epsilon_i^n \geq 0$. We also denote by $\tilde{V}_k^{n+1} = V_k^{n+1} + \epsilon_k^{n+1}$, for $\epsilon_k^{n+1} \geq 0$ and $k \in N_i$. Then the difference between the two sides of the inequality (24) is

$$\begin{aligned} T &:= g_i \left(\tilde{V}_i^{n+1}, \{\tilde{V}_k^{n+1}\}_{k \in N_i}, V_i^n \right) - g_i \left(V_i^{n+1}, \{V_k^{n+1}\}_{k \in N_i}, V_i^n \right) \\ &= \left(\frac{1}{\Delta t} + r \right) \epsilon_i^{n+1} - \frac{\tilde{\Sigma}^2}{2} \cdot \left(\delta_h^2 \tilde{V}_i^{n+1} - \delta_h \tilde{V}_i^{n+1} \right) + \frac{\hat{\Sigma}^2}{2} \cdot \left(\delta_h^2 V_i^{n+1} - \delta_h V_i^{n+1} \right) \\ &= \left(\frac{1}{\Delta t} + r \right) \epsilon_i^{n+1} - \frac{\tilde{\Sigma}^2}{2} \cdot \left(\delta_h^2 \tilde{V}_i^{n+1} - \delta_h \tilde{V}_i^{n+1} \right) + \frac{\tilde{\Sigma}^2}{2} \cdot \left(\delta_h^2 V_i^{n+1} - \delta_h V_i^{n+1} \right) \\ &\quad + \frac{\hat{\Sigma}^2}{2} \cdot \left(\delta_h^2 V_i^{n+1} - \delta_h V_i^{n+1} \right) - \frac{\tilde{\Sigma}^2}{2} \cdot \left(\delta_h^2 V_i^{n+1} - \delta_h V_i^{n+1} \right) \\ &\geq \left(\frac{1}{\Delta t} + r + \frac{\Sigma^2}{h^2} \right) \epsilon_i^{n+1} \geq 0, \end{aligned}$$

since $\frac{\tilde{\Sigma}^2}{2} \cdot \left(\delta_h^2 \tilde{V}_i^{n+1} - \delta_h \tilde{V}_i^{n+1} \right) \geq \frac{\hat{\Sigma}^2}{2} \cdot \left(\delta_h^2 \tilde{V}_i^{n+1} - \delta_h \tilde{V}_i^{n+1} \right)$, where

$$\tilde{\Sigma} = \Sigma \left(\delta_h^2 \tilde{V}_i^{n+1} - \delta_h \tilde{V}_i^{n+1} \right), \quad \hat{\Sigma} = \Sigma \left(\delta_h^2 V_i^{n+1} - \delta_h V_i^{n+1} \right).$$

We now turn to the perturbation on $\{V_k^{n+1}\}_{k \in N_i}$ and V_i^n . Then the difference between the

two sides of the inequality (25) is

$$\begin{aligned}
T' &:= g_i \left(V_i^{n+1}, \{\tilde{V}_k^{n+1}\}_{k \in N_i}, \tilde{V}_i^n \right) - g_i \left(V_i^{n+1}, \{V_k^{n+1}\}_{k \in N_i}, V_i^n \right) \\
&= -\frac{\epsilon_i^n}{\Delta t} - r \delta_h \tilde{V}_i^{n+1} + r \delta_h V_i^{n+1} - \frac{\tilde{\Sigma}^2}{2} \cdot \left(\delta_h^2 \tilde{V}_i^{n+1} - \delta_h \tilde{V}_i^{n+1} \right) + \frac{\hat{\Sigma}^2}{2} \cdot \left(\delta_h^2 V_i^{n+1} - \delta_h V_i^{n+1} \right) \\
&= -\frac{\epsilon_i^n}{\Delta t} - r \delta_h \tilde{V}_i^{n+1} + r \delta_h V_i^{n+1} - \frac{\tilde{\Sigma}^2}{2} \cdot \left(\delta_h^2 \tilde{V}_i^{n+1} - \delta_h \tilde{V}_i^{n+1} \right) + \frac{\hat{\Sigma}^2}{2} \cdot \left(\delta_h^2 \tilde{V}_i^{n+1} - \delta_h \tilde{V}_i^{n+1} \right) \\
&\quad + \frac{\hat{\Sigma}^2}{2} \cdot \left(\delta_h^2 V_i^{n+1} - \delta_h V_i^{n+1} \right) - \frac{\hat{\Sigma}^2}{2} \cdot \left(\delta_h^2 \tilde{V}_i^{n+1} - \delta_h \tilde{V}_i^{n+1} \right) \\
&\leq -\frac{1}{\Delta t} \epsilon_i^n - \left(\frac{r}{2h} + \frac{\hat{\Sigma}^2}{2h^2} - \frac{\hat{\Sigma}^2}{4h} \right) \epsilon_{i+1}^{n+1} - \left(\frac{\hat{\Sigma}^2}{2h^2} - \frac{r}{2h} + \frac{\hat{\Sigma}^2}{4h} \right) \epsilon_{i-1}^{n+1}.
\end{aligned}$$

If condition $h \leq \frac{2\underline{\Sigma}^2}{\max(2r - \underline{\Sigma}^2, \underline{\Sigma}^2 - 2r)}$ is satisfied, then we obtain $T' \leq 0$. The monotonicity of scheme (19) now follows directly from Definition 4.1. \square

Lemma 4.6. (Stability) *If condition $h \leq \frac{2\underline{\Sigma}^2}{\max(2r - \underline{\Sigma}^2, \underline{\Sigma}^2 - 2r)}$ is satisfied, then the fully implicit scheme (22) is stable, in the sense that*

$$\max_n \|V^n\|_\infty \leq \max \left(\|\phi\|_\infty, \max_n |\varphi^n| \right). \quad (48)$$

Proof. With the diagonal-dominated assumption, the maximum principle holds for the system (22). Moreover, the maximum value cannot be achieved at the left boundary. The estimate on l_∞ (48) follows directly. \square

Theorem 4.4. (Convergence to the viscosity solution) *If condition $h \leq \frac{2\underline{\Sigma}^2}{\max(2r - \underline{\Sigma}^2, \underline{\Sigma}^2 - 2r)}$ is satisfied, then the implicit scheme (22) converges to the viscosity solution of the nonlinear PDE (18).*

Proof. The proof process is the same as that in Theorem 4.1, and thus, it will not be reiterated here. \square

Theorem 4.5. (Rate of convergence) *Let v be the viscosity solution of equation (18), V be the numerical solution of equation (22). If condition $h \leq \frac{2\underline{\Sigma}^2}{\max(2r - \underline{\Sigma}^2, \underline{\Sigma}^2 - 2r)}$ is satisfied and there exists some $\beta \in (0, 1)$, such that $v \in C^{1+\beta/2, 2+\beta}([0, T] \times \Omega)$, then*

$$\max_n \|v^n - V^n\|_\infty \leq C \left(\Delta t^{\frac{\beta}{2}} + h^\beta \right), \quad (49)$$

where C is a positive constant independent of Δt and h .

Proof. Rate of convergence follows using the same steps as in Theorem 4.2 and Pei et al. [11]. \square

5. Numerical Examples

5.1. Butterfly Spread

To assess the performance of the proposed numerical methods, we first consider a butterfly spread, a standard benchmark for nonlinear option pricing models due to its non-convex payoff. The payoff function is defined as:

$$\phi(S) = \max(S - K_1, 0) - 2 \max(S - K_m, 0) + \max(S - K_2, 0), \quad (50)$$

where $K_m = (K_1 + K_2)/2$. Through the logarithmic transformation $X = \ln S$, we solve the PDE (18) with the transformed initial condition:

$$\phi(X) = \max(e^X - K_1, 0) - 2 \max(e^X - K_m, 0) + \max(e^X - K_2, 0). \quad (51)$$

For this test, we adopt the parameters from the benchmark problem in Pooley et al. [9]: $T = 0.25$, $r = 0.1$, $K_1 = 90$, $K_2 = 110$, $\underline{\Sigma} = 0.15$, and $\bar{\Sigma} = 0.25$. Our objective is to compute the option value at the at-the-money point $S_0 = 100$, which corresponds to $X = \ln(100)$ in the transformed domain.

Table 1: Convergence results for butterfly spread using the explicit finite difference scheme.

Timesteps	Spatial nodes	L^∞ error	Conv. rate	CPU time (s)
16	161	1.196	–	0.0087
64	321	3.858×10^{-1}	1.63	0.0118
256	641	1.031×10^{-1}	1.90	0.0146
1024	1281	2.499×10^{-2}	2.04	0.0354

To observe the convergence of our numerical methods, we compute numerical solutions on a sequence of progressively refined grids. The coarsest grid uses 161 uniform spatial points. At each subsequent refinement level, the number of spatial points is doubled, and the time step is quartered to maintain a consistent relationship. The convergence rate is computed using the formula

$$\text{Convergence rate} = \frac{\ln(E_{\text{coarse}}/E_{\text{fine}})}{\ln(r)}, \quad (52)$$

where E_{coarse} and E_{fine} are the L^∞ errors on consecutive grid levels, and $r = 2$ is the refinement ratio for spatial discretization. A high-resolution numerical solution computed on an exceptionally fine grid serves as the reference ("exact") solution for error estimation. Table 1 reports the convergence results for the explicit scheme, while Table 2 summarizes the results for the implicit scheme. For the implicit method, the nonlinear system at each time step is solved using the iterative scheme (23) with a convergence tolerance of 10^{-6} . The numerical results in Table 2 further show that the convergence of the implicit scheme does not require the mesh ratio condition $\bar{\Sigma}\sqrt{\Delta t} \leq h$.

Table 2: Convergence results for butterfly spread using the implicit finite difference scheme.

Timesteps	Spatial nodes	L^∞ error	Conv. rate	CPU time (s)
16	641	6.032×10^{-2}	–	0.2961
64	1281	1.565×10^{-2}	1.95	0.3198
256	2561	4.269×10^{-3}	1.87	0.4643
1024	5121	8.308×10^{-4}	2.36	1.9760

The convergence results in Tables 1 and 2 demonstrate that both schemes achieve approximately second-order accuracy. To evaluate the option value at the target point $X_0 = 2 \ln(10)$ (corresponding to $S_0 = 100$), which does not coincide with grid points, we employ quadratic Lagrange interpolation. Table 3 presents a comprehensive comparison of the convergence behavior for both explicit and implicit schemes.

Table 3: Option values at $X_0 = 2 \ln(10)$ using quadratic Lagrange interpolation for butterfly spread option.

Explicit Scheme				Implicit Scheme			
Steps	Nodes	Value	Difference	Steps	Nodes	Value	Difference
16	161	5.757737	8.762×10^{-1}	16	641	4.895220	1.372×10^{-2}
64	321	4.906351	2.485×10^{-2}	64	1281	4.883320	1.738×10^{-3}
256	641	4.879003	2.579×10^{-3}	256	2561	4.882627	1.045×10^{-3}
1024	1281	4.883390	1.808×10^{-3}	1024	5121	4.881922	3.400×10^{-4}

Reference value: 4.881582, computed via implicit scheme with 16384 temporal and 20481 spatial grid points.

Figure 1 illustrates the convergence behavior of the inner iteration scheme for the implicit method. It can be seen that the number of iterations per time step is almost always only 2, demonstrating the high efficiency of the implicit numerical algorithm.

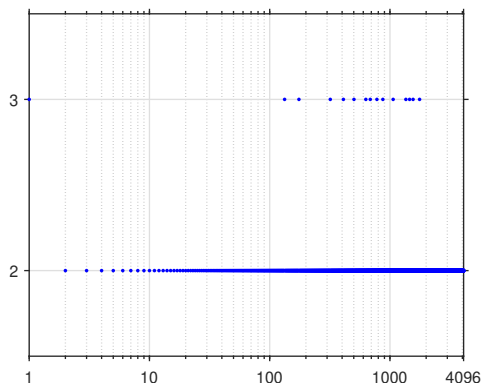


Figure 1: The number of iterations within each time step.

5.2. Digital Call Option

To further test the robustness of our schemes, we consider a digital call option, which presents a more significant challenge due to its discontinuous payoff at the strike price K :

$$U(T, S) = \begin{cases} 1 & \text{if } S \geq K, \\ 0 & \text{if } S < K, \end{cases} \quad (53)$$

The parameters for this test case are also adopted from Pooley et al. [9], with $T = 0.25$, $r = 0.1$, $K = 100$, $\underline{\Sigma} = 0.15$, and $\bar{\Sigma} = 0.25$.

Through the logarithmic transformation $X = \ln S$, we solve the PDE (18) with the transformed initial condition:

$$\phi(X) = \begin{cases} 1 & \text{if } e^X \geq K, \\ 0 & \text{if } e^X < K. \end{cases} \quad (54)$$

Table 4: Convergence results for the digital call option using the explicit finite difference scheme.

Timesteps	Spatial nodes	L^∞ error	Conv. rate	CPU time (s)
64	961	4.142×10^{-2}	–	0.0093
256	1921	1.989×10^{-2}	1.06	0.0210
1024	3841	9.209×10^{-3}	1.11	0.0599
4096	7681	3.908×10^{-3}	1.24	0.3246

Table 5: Convergence results for the digital call option using the implicit finite difference scheme.

Timesteps	Spatial nodes	L^∞ error	Conv. rate	CPU time (s)
64	1281	1.195×10^{-2}	–	0.0468
256	2561	2.238×10^{-3}	0.62	0.2089
1024	5121	5.483×10^{-3}	0.73	1.6998
4096	10241	1.836×10^{-3}	1.19	14.1552

Tables 4 and 5 present the convergence results for the explicit and implicit schemes, respectively. As anticipated, the discontinuity in the payoff function degrades the performance of both numerical schemes. The lack of regularity in the terminal condition reduces the global smoothness of the PDE’s viscosity solution. Consequently, as shown in Tables 4 and 5, the empirical convergence rates are markedly lower than those for the butterfly spread, approaching first-order accuracy. To evaluate the option value at the target point $X_0 = 2 \ln(10)$ (corresponding to $S_0 = 100$), we again employ quadratic Lagrange interpolation. A detailed comparison of the convergence behavior for both schemes is presented in Table 6.

Table 6: Option values at $X_0 = 2 \ln(10)$ using quadratic Lagrange interpolation for digital call option.

Explicit Scheme				Implicit Scheme			
Steps	Nodes	Value	Difference	Steps	Nodes	Value	Difference
64	961	0.652812	3.785×10^{-2}	64	1281	0.703109	1.245×10^{-2}
256	1921	0.673527	1.714×10^{-2}	256	2561	0.688523	2.139×10^{-3}
1024	3841	0.683729	6.933×10^{-3}	1024	5121	0.696152	5.490×10^{-3}
4096	7681	0.688773	1.889×10^{-3}	4096	10241	0.692500	1.838×10^{-3}

Reference value: 0.690662, computed via implicit scheme with 16384 temporal and 20481 spatial grid points.

Figure 2 illustrates the convergence behavior of the inner iteration scheme for the implicit method, showing similar efficiency to the butterfly spread case with consistently low iteration counts per time step.

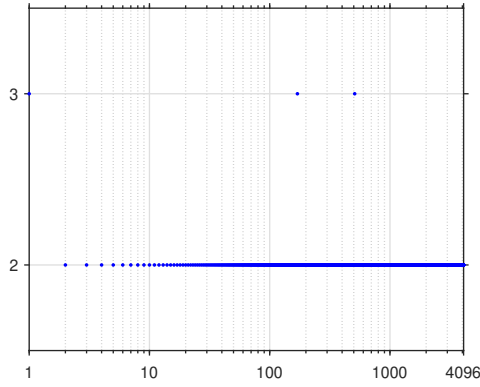


Figure 2: The number of iterations within each time step.

5.3. Benefits of Logarithmic Transformation

As detailed in Remark 4.1, a key motivation for the logarithmic transformation $X = \ln S$ is to relax the restrictive stability constraint of the explicit finite difference scheme. To quantify this theoretical advantage, we conduct a direct numerical comparison between solving the G-option equation in the original S -domain and the transformed X -domain.

Experimental Design. To ensure a fair comparison, both formulations are solved using the same number of spatial grid points ($M = 200, 400, 800$). The computational domain for the original formulation is set to $[S_{\min}, S_{\max}] = [50, 150]$, corresponding to $[X_{\min}, X_{\max}] = [\ln(50), \ln(150)]$ for the log-transformed problem. For each value of M , we determine the minimum number of time steps required by the stability condition for the explicit scheme in each domain.

Tables 7 and 8 present the numerical results for both schemes at different levels of grid refinement. The results provide quantitative evidence of the improvement achieved through

the logarithmic transformation. The grid ratio (for time discretization) of the numerical scheme with logarithmic transformation is approximately 2.7155 times lower than that without the transformation.

Table 7: Comparison of numerical results for the butterfly spread option with and without logarithmic transformation. Reference value $V_{\text{ref}} = 4.881540$ obtained by the implicit scheme with 16384 temporal and 20481 spatial steps (logarithmic transform).

	$M = 200$		$M = 400$		$M = 800$	
	Without log	With log	Without log	With log	Without log	With log
Spatial step size	5.00×10^{-1}	5.49×10^{-3}	2.50×10^{-1}	2.75×10^{-3}	1.25×10^{-1}	1.37×10^{-3}
Minimum time step	1.41×10^3	5.18×10^2	5.63×10^3	2.07×10^3	2.25×10^4	8.29×10^3
Numerical solution	4.88397	4.88094	4.88215	4.88127	4.88169	4.88142
Relative error	4.97×10^{-4}	1.23×10^{-4}	1.24×10^{-4}	5.47×10^{-5}	3.03×10^{-5}	2.42×10^{-5}
CPU time (s)	1.80×10^{-2}	1.12×10^{-2}	4.77×10^{-2}	3.34×10^{-2}	2.06×10^{-1}	8.80×10^{-2}

Table 8: Comparison of numerical results for the digital option with and without logarithmic transformation. Reference value $V_{\text{ref}} = 0.690660$ obtained by the implicit scheme with logarithmic transformation using 16384 temporal and 20481 spatial steps.

	$M = 200$		$M = 400$		$M = 800$	
	Without log	With log	Without log	With log	Without log	With log
Spatial step size	5.00×10^{-1}	5.49×10^{-3}	2.50×10^{-1}	2.75×10^{-3}	1.25×10^{-1}	1.37×10^{-3}
Minimum time step	1.41×10^3	5.18×10^2	5.63×10^3	2.07×10^3	2.25×10^4	8.29×10^3
Numerical solution	6.8029×10^{-1}	6.8470×10^{-1}	6.8514×10^{-1}	6.8928×10^{-1}	6.8755×10^{-1}	6.9156×10^{-1}
Relative error	1.50×10^{-2}	8.63×10^{-3}	7.99×10^{-3}	2.00×10^{-3}	4.50×10^{-3}	1.36×10^{-3}
CPU time (s)	3.86×10^{-2}	1.19×10^{-2}	7.08×10^{-2}	3.17×10^{-2}	2.03×10^{-1}	8.59×10^{-2}

The numerical investigations underscore several critical advantages of employing the logarithmic transformation in the context of explicit difference schemes for G-option pricing equations:

- **Relaxed Stability Constraint:** The transformation significantly loosens the stability condition inherent in explicit schemes. For instance, with $M = 800$ spatial points, the minimum number of time steps required in the original S -domain is 22500, whereas the transformed X -domain requires only 8286—a reduction of approximately 63%.
- **Improved Computational Efficiency:** Consequently, the log-transformed approach achieves comparable or superior accuracy at a substantially lower computational cost. As shown in the CPU time comparisons, the efficiency gains become more pronounced as the grid is refined.

These results collectively establish the logarithmic transformation as a highly practical and theoretically justified preprocessing technique, which can be used for robust and efficient numerical processing of the G-option equation.

6. Conclusions

We have established the risk-neutral pricing problem of options under the G-expectation and developed explicit and implicit discretization schemes respectively to solve it. First, we describe the price of the underlying asset through the G-geometric Brownian motion, propose a risk-neutral pricing model for options under the G-expectation, and then derive the G-Black-Scholes equation. To improve computational efficiency and reduce numerical cost, we introduce a logarithmic transformation of the asset price and obtain an alternative nonlinear PDE. Then, we demonstrate the consistency, stability, and monotonicity of the two numerical schemes respectively. In particular, for the implicit scheme, we prove the monotonic convergence of the nonlinear inner iteration at each time step. In addition, we provide an estimate of the convergence order. Finally, the numerical examples we present further confirm the accuracy and computational advantages of the proposed methods.

Acknowledgments

This work of Yue was partially supported by the NSFC Grant 12371401. This work of Zheng was partially supported by the Postgraduate Research & Practice Innovation Program of Jiangsu Province (Grant No. KYCX25 3502).

References

- [1] L.B.G. Andersen, R. Brotherton-Ratcliffe, The equity option volatility smile: an implicit finite-difference approach, *J. Comput. Finance* 1(2) (1998) 5–37.
- [2] M. Avellaneda, A. Levy, A. Parás, Pricing and hedging derivative securities in markets with uncertain volatilities, *Appl. Math. Finance* 2(2) (1995) 73–88.
- [3] F. Black, M. Scholes, The pricing of options and corporate liabilities, *J. Polit. Econ.* 81(3) (1973) 637–654.
- [4] G. Barles, P.E. Souganidis, Convergence of approximation schemes for fully non-linear second order equations, *Asymptot. Anal.* 4(3) (1991) 271–283.
- [5] T.F. Coleman, Y. Li, A. Verma, Reconstructing the unknown local volatility function, *J. Comput. Finance* 2 (1999) 77–102.
- [6] L. Denis, C. Martini, A theoretical framework for the pricing of contingent claims in the presence of model uncertainty, *Ann. Appl. Probab.* 16(2) (2006) 827–852.
- [7] S.L. Heston, A closed-form solution for options with stochastic volatility with applications to bond and currency options, *Rev. Financ. Stud.* 6(2) (1993) 327–343.
- [8] T.J. Lyons, Uncertain volatility and the risk-free synthesis of derivatives, *Appl. Math. Finance* 2(2) (1995) 117–133.

- [9] D.M. Pooley, P.A. Forsyth, K.R. Vetzal, Numerical convergence properties of option pricing PDEs with uncertain volatility, *IMA J. Numer. Anal.* 23(2) (2003) 241-267.
- [10] K. Ma, P.A. Forsyth, An unconditionally monotone numerical scheme for the two-factor uncertain volatility model, *IMA J. Numer. Anal.* 37(2) (2017) 905-944.
- [11] Z.T. Pei, X.Y. Yue, X.T. Zheng, Numerical methods for two-dimensional G-heat equation, arXiv:2503.02395, 2025.
- [12] S. Peng, G-expectation, G-Brownian motion and related stochastic calculus of Ito's type, *Stochastic analysis and applications*, 541-567, Abel Symp., 2, Springer, 2007.
- [13] S. Peng, *Nonlinear expectations and stochastic calculus under uncertainty with robust CLT and G-Brownian motion*. Springer, 2019.
- [14] Y. Xin, H. Zheng, Black-Scholes model under G-Lévy Process, *J. Appl. Math. Phys.* 9(12) (2021) 3202-3210.
- [15] Y. Xu, Y. Li, Option pricing model driven by G-Lévy process under the G-expectation framework, *J. Appl. Math. Phys.* 11(1) (2023) 46-54.